Monte Carlo Simulation in Thermal Radiative Transfer: Method Review, Validation and Parameter Sensitivity

Zafar U. Koreshi, Sadaf Siddiq, Tasneem M. Shah[1]

Abstract—**Monte Carlo (MC) simulation is extensively used for solving thermal radiation problems in high-temperature environments, such as combustion chambers and furnaces, and irregular-geometry enclosures containing participative media such as combustive gases. The quantities of interest are surface radiosities and subsequent radiative heat fluxes which have been accurately determined by MC in configurations which are challenging for deterministic formulations. The attractiveness of MC schemes becomes more prominent in mixed-mode and coupled thermo-fluid problems, where the non-linearity, spectral characteristics and geometrical complexity may render deterministic treatments largely ineffective. This work deals with thermal radiative estimates for hot grey diffuse surfaces and grey participative media. Simple test-configurations are considered for which exact solutions are available and MC simulation is used to make validation comparisons. We also consider the analog simulation process to compute sensitivities of independent parameter variations, such as material density, in a single simulation. Such a capability increases the applicability of MC methods to optimization studies as easily as deterministic methods based on variational schemes.**

***Index Terms*— Mixed-mode heat transfer, Monte Carlo simulation, participating media, Stochastic sensitivity, Thermal radiation.**

I. Introduction

MONTE CARLO (MC) simulation has been extensively used for solving thermal radiation problems in high-temperature environments including combustion chambers and furnaces, and irregular-geometry enclosures containing participative media such as combustive gases. Surface radiosities and subsequent heat fluxes have been accurately determined in configurations which are difficult for deterministic formulations. The attractiveness of MC schemes becomes more prominent in mixed-mode and coupled thermo-fluid problems, where the non-linearity, spectral characteristics and geometrical complexity may render deterministic treatments largely ineffective.

This work deals with thermal radiative estimates for hot grey diffuse surfaces and grey participative media. Simple test-configurations are considered for which the exact solutions are available and MC simulation is used to make validation comparisons. We consider two problems *viz* (i) a two-surface source-sink infinite configuration, and (ii) an enclosure with fixed-temperature surfaces.

Three methods -- an electric circuit analogy model, a deterministic integral formulation, and a Monte Carlo simulation model -- are used to estimate the radiative heat flux and in some cases, the temperature distribution.

The MC simulation is based on tracking the history of bundles of photons from 'birth', as emitted photons, to 'death' when they are absorbed at a surface or within a participative medium. We consider the accuracy and precision of MC estimates as a function of the number of photon bundles sampled and the radiative properties of surfaces. Surface radiosities are determined from surface irradiations in scattering events. The accuracy of MC estimates, known to depend strongly on both the geometry and emissivity, is quantified for the test configurations. From this, we are able to obtain estimates of the required sample size for simulation. Similarly, the emissivity data for surfaces determines the events in a history. Strong absorption at a surface, for example, terminates a history before it makes a 'significant' contribution to a tally of interest at the other surface. Such an 'analog' MC simulation is bound to give significant errors and hence requires modification by one or several methods.

In the last part of the paper, we consider sensitivity capabilities of MC simulation to obtain perturbations in estimates of radiative heat flux due to independent variation in material properties. For this, improvement strategies such as artificially altering, or biasing, the underlying probability distribution function (PDF) to force more events in the simulation and 'correct' the statistical tally are demonstrated to give a 'better' estimate. The simplicity of the test configurations allows us to write simple terms for the

[1] Dr. Zafar Ullah Koreshi is a Professor at Air University, Islamabad, Pakistan (Ph: 0092(345)5115936; fax: 0092(51)9260158; e-mail: zafar@mail.au.edu.pk.)

Engr. Sadaf Siddiq is an Assistant Professor at Air University, Islamabad, Pakistan. (Ph: 0092(333)5637932; fax: 0092(51)9260158 ; e-mail: sadaf@mail.au.edu.pk.)

Dr. Tasneem M. Shah is a Professor at Air University, Islamabad, Pakistan. (Ph: 0092(300)5269610; fax: 0092(51)9260158; e-mail: dr.tasneem@mail.au.edu.pk.)

probabilities of events based on the multiple scattering of photons from surfaces. We are thus able to quantify the effect of such a technique in a simulation of a simple configuration and to infer on the validity of such a scheme in complex problems. It is anticipated that this work will demonstrate ways of obtaining better MC estimates more efficiently, *i.e.* without excessive computational effort, and will be extended to non-grey surfaces and participative media.

II. Deterministic and Stochastic Methods

A. The Electric Circuit Analogy Method

In an elementary deterministic "circuit diagram" analogy, the net heat flow can be expressed [1], [2] as

$$\dot{Q} = \frac{e_{b_1} - q_1^+}{R_1} = \frac{q_1^+ - q_2^+}{R_2} = \frac{q_2^+ - e_{b_2}}{R_1} \quad , \tag{1}$$

and an "overall" flow between surface 1 and 2 can then be written as

$$\dot{Q} = \frac{e_{b_1} - e_{b_2}}{\sum_{i=1}^{3} R_i} \quad , \tag{2}$$

where the resistances are given by

$$R_1 = \frac{1-\varepsilon_1}{\varepsilon_1 A_1}, R_2 = \frac{1}{A_1 F_{12}}, R_3 = \frac{1-\varepsilon_2}{\varepsilon_2 A_2} \, . \tag{3}$$

Here, the view factor F_{12} is

$$F = \frac{2}{\pi x Y}\left\{ \begin{array}{l} \ln\left[\frac{(1+X^2)(1+Y^2)}{(1+X^2+Y^2)}\right]^{1/2} + X\sqrt{1+Y^2}\tan^{-1}\left(\frac{X}{\sqrt{1+Y^2}}\right) + \\ Y\sqrt{1+X^2}\tan^{-1}\left(\frac{Y}{\sqrt{1+X^2}}\right) - X\tan^{-1}X - Y\tan^{-1}Y \end{array} \right\} \tag{4}$$

where $X \equiv a/D, Y \equiv b/D$ (*a*, *b* are length and width of plates respectively and *D* is the distance between the plates).

B. Integral Formulation

We can also write an integral equation for the net heat flux in a gray, diffuse enclosure is [2],[3] as

$$\frac{q(r)}{\varepsilon(r)} - \int_{A'} \left(\frac{1}{\varepsilon(r')} - 1\right) q(r') dF_{dA \to dA'} = e_b(r) - \int_{A'} e_b(r') dF_{dA \to dA'} \, . \tag{5}$$

For two surfaces of length *a*, width *b* separated by distance *D* two equations can be written from Eqn.(5). For coordinates x_1 and x_2 are taken along the surfaces and using

$$dx_1 dF_{dx_1 \to dx_2} = dx_2 dF_{dx_2 \to dx_1} = \frac{D^2}{2} \frac{dx_1 dx_2}{[D^2 + (x_2 - x_1)^2]^{3/2}}$$

, the differential view factors can be found. The thermal flux equations, for isothermal surfaces, are then:

$$\frac{q_1(\xi_1)}{\varepsilon_1} - \left(\frac{1}{\varepsilon_2} - 1\right) \int_0^{a/D} q_2(\xi_2) f(\xi_1, \xi_2) d\xi_2 \tag{6.a}$$

$$= e_{b,1} - e_{b,2} \int_0^{a/D} f(\xi_1, \xi_2) d\xi_2$$

and

$$\frac{q_2(\xi_2)}{\varepsilon_2} - \left(\frac{1}{\varepsilon_1} - 1\right) \int_0^{a/D} q_1(\xi_1) f(\xi_1, \xi_2) d\xi_1 = \tag{6.b}$$

$$e_{b,2} - e_{b,1} \int_0^{a/D} f(\xi_1, \xi_2) d\xi_1$$

for $\xi \equiv x/D$ and $f(\xi_1, \xi_2) \equiv \frac{1}{2\left[1 + (\xi_2 - \xi_1)^2\right]^{3/2}}$.

Consider now the integral formulation for a participating non-scattering medium between parallel plates. The integro-differential equation is [3]

$$\frac{dI_\eta}{d\tau_\eta} + I_\eta = S_\eta(\tau_q, \hat{s}) \tag{7}$$

where the source term is given by

$$S_\eta(\tau_q, \hat{s}) = (1 - w_\eta) I_{b,\eta} + \frac{\omega_\eta}{4\pi} \int_{4\pi} I_\eta(\hat{s}_i) \Phi_\eta(\hat{s}_i, \hat{s}) d\Omega_i \, . \tag{7.a}$$

If the source function is known, equation (7) can be integrated and the intensity can be found as

$$I_\eta(\tau_\eta) = I_\eta(0) e^{-\tau_\eta} + \int_0^{\tau_\eta} S_\eta(\tau'_\eta, \hat{s}) e^{-(\tau_\eta - \tau'_\eta)} d\tau'_\eta \tag{8}$$

where τ'_η is the optical coordinate. We consider the simple cases of two infinite plane surfaces with a non-scattering participating medium. We assume that collisions in the participating medium are all absorptions and an absorption results in a blackbody emission [2]. Writing the angular dependence explicitly, equation (8) is

$$I(t, \mu) = I(0, \mu) \exp(-t/\mu) + \int_0^t I_b(t') \exp\left(\frac{t' - t}{\mu}\right) \frac{dt'}{\mu} \tag{9}$$

and separating the forward and backward components of the intensity $I^+(t, \mu > 0)$ and $I^-(t, \mu < 0)$ we can write the radiosities from surface 1 and surface 2 as

$$q_1^+ \equiv \int_{\theta=0}^{\pi/2} \cos\theta d\mu \int_0^{2\pi} I(\theta, \phi) d\phi = \pi I^+(0) \, , \tag{10.a}$$

and

$$q_2^- \equiv \int_{\theta=\pi/2}^{\pi} \cos\theta d\mu \int_0^{2\pi} I(\theta, \phi) d\phi = \pi I^-(t_L) \, . \tag{10.b}$$

The above quantities can be used to find the forward and backward intensities in the medium $I^+(t, \mu)$ and $I^-(t, \mu)$ respectively. From these, the forward and backward fluxes $q^+(t)$ and $q^-(t)$ respectively can be found, and the net flux $q(t) \equiv q^+(t) - q^-(t)$. From the steady-state energy equation, for conduction of thermal radiation, we know

that $dq/dt = 0$. Using Leibnitz's Rule and relationships for exponential integral functions

$$E_n(t) = \int_0^1 \mu^{n-2} \exp(-t/\mu) d\mu ,$$

and defining non-dimensional quantities for the temperature field and the radiative heat flux as

$$e_b^* \equiv \frac{e_b(t) - q_2^-}{q_1^+ - q_2^-}$$

and

$$q^* \equiv \frac{q}{q_1^+ - q_2^-},$$

the resulting equations are:

$$2e_b^* = E_2(t) + \int_0^{t_L} e_b^*(t') E_1(|t - t'|) dt' , \quad (11.a)$$

and

$$q^* = 1 - 2\int_0^{t_L} e_b^*(t') E_2(t') dt' . \quad (11.b)$$

The quantities above, e_b^* and q^* can be found by solving the integral equations (11); however to find the unknowns, $e_b(t)$ and q require that the surface radiosities are known. If the surface temperatures only are known, then the radiosity terms have to be replaced by the known quantities. This is achieved from the relations. The final results are then:

$$\frac{e_b(t) - e_{b,2}}{e_{b,1} - e_{b,2}} = \frac{e_b^*(t) + \frac{1-\varepsilon_2}{\varepsilon_2} q^*}{1 + q^*(\frac{1}{\varepsilon_1} + \frac{1}{\varepsilon_2} - 2)}, \quad (12)$$

and

$$q = \frac{q^*(e_{b,1} - e_{b,2})}{1 + \left(\frac{1-\varepsilon_1}{\varepsilon_1} + \frac{1-\varepsilon_2}{\varepsilon_2}\right) q^*} . \quad (13)$$

C. Monte Carlo Simulation

We now consider a simulation method based on following the photons as they travel from birth to their final destination. The Monte Carlo (MC) simulation [2],[5] consists of sampling "source" bundles from one surface and transporting them to their final destination using laws of probability. A simulation of *N* histories involves the following steps for a history

i. Specification of the source emissive power.
ii. Selection of emission angles θ and φ.
iii. Ray tracing in the direction of propagation.
iv. Determination of point of intersection, if any with the destination surface.
v. Determination of fate of history at the destination surface.

The vector of propagation $\hat{S}$ is related to the unit vectors $\hat{t}_1, \hat{t}_2$ and $\hat{n}$. In the direction $\hat{S}$, the point of intersection Q can be found as follows: The sample size is determined from the emitted energy of a surface, $E = A\varepsilon e_b \equiv A\varepsilon\sigma T^4$ Watts. One selects *N* bundles, each bundle having energy ω such that $E = \omega N$. In case of two surfaces, the energy per bundle can be kept constant so that $\omega_1 = \frac{E_1}{N_1} = \omega_2 = \frac{E_2}{N_2}$.

With surface 1 as the "reference surface", the number of bundles started from surfaces is kept as $N_2 = (\frac{E_2}{E_1})N_1$. The point of emission p_e from a surface is determined as

$$x_e = \xi_1(x_{\max} - x_{\min}) + x_{\min}$$

$$y_e = \xi(y_{\max} - y_{\min}) + y_{\min}$$

The polar and azimuthal angles θ and φ respectively are then determined as $\theta = \sin^{-1}(\sqrt{\xi_3})$ for a diffuse surface emitter, and $\phi = 2\pi\xi_4$. On intersection at Q, a scattering is chosen with probability $1-\varepsilon$ and thus $0 < \xi_5 \le 1-\varepsilon$ determines a scattering whereas $1-\varepsilon < \xi_5 \le 1$ corresponds to an absorption. In case of scattering, new angles θ φ are determined and the process continues until the history is terminated on absorption. The quantity of interest in the problem is the energy exchange or equivalently, the difference between the energy emitted from a surface and absorbed by that surface.

This can indeed be generated to an *N*-Surface configuration

$$q_1^+ = \varepsilon_1 e_{b_1} - \rho_i q \sum_{j=1}^{N} F_{ij} q_j^+$$

and includes the "self-contribution" $F_{ijq}q_i^+$ which may be non-zero for a re-entrant surface. The quantities of interest are q^+ and q^- which are determined with ε, e_b specified in the material data. Tally counter counts are updated each time a surface absorption, or emission takes place. Since the present configuration consists of gray surfaces, a spectral index is not required.

The configuration considered in the following analysis has two black surfaces with a gray participating medium which has both absorption and scattering. The analysis leading to the expressions in the previous section for a purely absorbing medium also apply here, as scattering is taken to be an emission resulting from absorption in the participating medium. For simplicity, surface '2' is considered to be a zero temperature so that it does not emit any photons. The number of photon bundles started from surface 1 is $N_{w,1}$ and the energy per bundle is

$$w_1 = \sigma T_1^4 A_1 \Big/ N_{w,1} .$$

The normalized heat flux q^* is estimated from the number of photon bundles emitted from surface '1', and the number of photon bundles absorbed by each of the surfaces $S_{w,1}, S_{w,2}$ as

$$q^* = \frac{N_{w,1} - S_{w,1}}{N_{w,1}} \equiv \frac{S_{w,2}}{N_{w,1}}.$$

The distance to collision, s, is obtained from the PDF:

$$f(s)ds = K_t e^{-K_t s} ds,$$

from which, using a uniformly random number in the range (0,1) for the CDF, a distance to collision DTC, can be sampled as

$$s = -\frac{1}{K_t}\ln(1-\xi).$$

The average value of the DTC, or the mean free path $< s >$ is then

$$< s >= \int_0^\infty sf(s)ds = \frac{1}{K_t}.$$

Alternately, in units of optical distance, also called the optical depth, $t = K_t s$, the mean optical path is then $< t >= 1$.

III. Results

For the first validation exercise, we consider two parallel plates of dimensions 1*m* X 1*m*. The "exact" radiosity vales are obtained from the circuit diagram method and compared with MC simulation. Tables 1a and 1b shows the results from both methods for different sample size in MC computations.

TABLE 1A
CASES CONSIDERED FOR COMPARISON OF NET RADIATIVE HEAT FLUX FROM ELECTRICAL CIRCUIT ANALOGY AND MC ANALOG SIMULATION METHODS.

Case	N_b,N_1,N_2	T_1 (K)	T_2 (K)	ε_1	ε_2	D (m)
Set A	Q_{net}=0					
A1	10,10^3,10^3	2000	2000	1.0	1.0	1-5
A2	10,10^3,444	2000	2000	0.9	0.4	1-5
A3	10,10^3,111	2000	2000	0.9	0.1	1-5
Set B	Q_{net}=0					
B1	10,10^3,10^3	2000	2000	1.0	1.0	0.1
B2	10,10^3,444	2000	2000	0.9	0.4	0.5
B3	10,10^3,111	2000	2000	0.9	0.1	1.0
Set C	Q_{net}= 60.2 kW, 9.48 kW, 2.61 kW					
C1	10,10^3,7	2000	1000	0.9	0.1	1.0
C2	10,10^3,7	2000	1000	0.9	0.1	5.0
C3	10,10^3,7	2000	1000	0.9	0.1	10.
Set D	Q_{net}=10.1 kW, 10.1 kW					
D1	10,10^3,0	2000	500	0.9	0.1	5.0
D2	10,10^3,0	2000	250	0.9	0.1	5.0
D3	10,10^3,0	2000	125	0.9	0.1	5.0

Here, N_b, N_1, and N_2 are the batch size and the number of photons started from isothermal surfaces 1 and 2 at temperatures T_1, T_2 and emissivities $\varepsilon_1, \varepsilon_2$ respectively. Table 1.a. shows four sets of configurations (*A, B, C* and *D*) arranged in order of complexity. Set A has no net radiant transfer and touching surfaces, so that all started particles contact with the 'other' surface and ensure 'good' statistics. The number of photon bundles started at surface 1 (N_1) is chosen arbitrarily while N_2 is calculated from the condition requiring constant enrgy per bundle: $\omega_1 = \omega_2$ as described above. Set *D* is taken to be the 'worst' case in which the statistics is expected to be poor. For the configurations given in Table 1.a., the radiosity of each surface is computed using the exact the expression (Eqn. 1) and the MC simulation described in Section II, and listed in Table I.b. The results for the MC estimate show the mean value along with the standard deviation.

TABLE 1B
RADIOSITY COMPUTATIONS FOR CASES CONSIDERED FOR COMPARISON OF NET RADIATIVE HEAT FLUX FROM ELECTRICAL CIRCUIT ANALOGY AND MC ANALOG SIMULATION METHODS.

Case	Exact Radiosity		MC Radiosity	
	q_1^+	q_2^+	q_1^+	q_2^+
A1	9.07e5	9.07e5	9.07e5	9.07e5
A2	9.07e5	9.07e5	9.07e5±1.11e3	8.96e5±1.5e4
A3	9.07e5	9.07e5	9.07e5±8.65e2	8.99e5±7.0e4
B1	9.07e5	9.07e5	9.07e5±8.6e0	9.07e5±1.49e1
B2	9.07e5	9.07e5	8.40e5±1.1e3	5.72e5±1.97e4
B3	9.07e5	9.07e5	8.21e5±3.3e2	2.38e5±2.47e4
C1	9.00e5	5.99e5	8.19e5±5.5e2	1.77e5±2.96e4
C2	9.06e5	1.42e5	8.16e5±4.2e1	1.45e4±9.75e3
C3	9.07e5	8.02e4	8.16e5±2.7e1	7.14e3±2.94e3
D1	9.06e5	9.41e4	8.16e5±3.6e1	7.7e3±7.35e3
D2	9.06e5	9.12e4	8.16e5±2.7e1	4.43e3±4.87e3
D3	9.06e5	9.09e4	8.16e5±3.6e1	5.14e3±5.73e3

For the integral equation without a participating medium, we convert the integrals (equations 6) to an *N*th order Gaussian quadrature scheme

$$\int_{-1}^{1} f(\xi_1, \xi_2)d\xi_2 \cong \sum_{i=1}^{N} w_i f(\xi_1, t_i)$$

and

$$\int_{-1}^{1} f(\xi_1, \xi_2)d\xi_1 \cong \sum_{i=1}^{N} w_i f(t_i, \xi_2),$$

using the transformation

$$\xi = \frac{W}{2h}(y+1).$$

The system of equations is $\underline{\underline{A}}\,\underline{q} = \underline{b}$. In this second-order Gaussian quadrature scheme, the weights are $w_1 = w_2 = 1$, and the evaluations are made at $t_1 = -t_2 = 1/\sqrt{3}$. We obtain the normalized heat fluxes given in Table 2.

TABLE 2
NORMALIZED HEAT FLUXES
($W/H=1$, $T_1 = T_2 = 1000\ K$)

ε_1	ε_2	$\tilde{q}_i \equiv q_i / (\varepsilon_1 \sigma T_1^4)$			
		$\tilde{q}_1(t_1)$	$\tilde{q}_1(t_2)$	$\tilde{q}_2(t_1)$	$\tilde{q}_2(t_2)$
0.1	0.1	0.9388	0.9775	0.9388	0.9775
0.2	0.2	0.8825	0.9564	0.8825	0.9564
0.5	0.5	0.2341	0.1210	0.2070	0.0515
0.9	0.9	0.5900	0.8407	0.5900	0.8407

The results of Table 1.a. show that for Set A, the first test case represents two black surfaces, with same temperatures touching each other with 10 batches consisting of 1000 histories from each surface, the MC results match the exact results. The standard deviations are zero in this case, as is the net heat flux. All the "single event" histories consist of absorptions, no scatterings and no losses. In this sense, it is the easiest of the cases for a MC simulation. As the emissivity of the second surface decreases, the number of absorptions on this surface also decreases resulting in an increase in the error and in the standard deviation. The third run in Set A confirms the trend.

Set B is intended to quantify the error in the MC simulation due to a decrease in the view factor of the surface and hence an increase in the number of lost bundles. The accuracy of the lower emissivity surface drops due to the smaller sampled source as well as to the smaller number of absorptions on the second surface. The sharp decrease in the accuracy of the MC estimate for the third case in Set B is due to the lower emissivity of the second surface, and hence the smaller sample, and the larger loss term. In fact, out of 1111 photon bundles, the surface absorptions were 54 and 20 on surfaces 1 and 2 respectively while 1037 (93.34%) got lost. For this problem, the view factor is about 0.2 so that the about 80% of the emissions would be expected lost from the direct source.

Set C considers difficult configurations for an MC simulation in which the photon energy per bundle is kept constant. In fact, the first case of this set results in 32 and 23 absorptions on surfaces 1 and 2 respectively while 948 are lost (94%) compared with a view factor of about 0.2. The second case of this set has 0.3 and 1.2 surface absorptions respectively or 1.5% of the total while the view factor is about 1.2%. In the third case, the radiosity estimates are almost completely due to the emissions rather than from the interaction between the surfaces, which has reduced the net power exchange to only 2.61 kilowatts. Finally, Set D is the worst case for an MC simulation based on the current strategy of constant bundle energy.

The results of the deterministic integral formulation, as shown in Table 2 do not have any associated uncertainty other than the numerical error in the quadrature approximation but have the disadvantage that the quantities of interest are found at specific points only.

IV. APPLICATIONS

The engineering applications of radiative flux in furnaces and 2-D and 3-D enclosures, have been obtained by MC simulations and validated experimentally, (see *e.g.* [4]).

The work is also extensively used for studying the effect of Thermal Barrier Coatings (TBC) which are used to reduce the heat flux on a surface so that it may perform according to the requirements. In an engine, for example, a 150 μm thick coating of yttria stabilized zirconia coating can cause a temperature drop of 170 C. Similarly, converging-diverging nozzles can be protected by similar TBCs.

The surface flux in a combustion chamber, for example, can be found here using the integral formulation with a participating medium. We consider two parallel plates of given temperatures and emissivities, separated by a non-scattering medium. The temperature field $T(t) = f(e_b(T))$ between the plates and the net radiative thermal flux q can be determined, for which the exact results are given by equations (12) and (13). Table 3 shows the design requirement for cooling rate required to keep surface 2 at the prescribed temperature. This will remove the heat found as the net thermal radiative flux. Surface 1 is thus a 'source condition' while surface 2 represents a sink. The engineering design problem can be to find the material corresponding to a specified absorption coefficient if plate spacing is fixed, or alternately to find the plate spacing if the material is given.

TABLE 3
COOLING RATE* (Q_c) REQUIRED TO KEEP SURFACE 2 AT THE TEMPERATURE T_2 K.

Surface 1		Surface 2		Opt.Th.	q^*	q
T_1/K	ε_1	T_2/K	ε_2	$t \equiv K_a L$		$W.cm^{-2}$
2000	0.1	400	0.9	0	1.00	8.47
2000	0.1	400	0.9	2.5	0.34	7.52
2000	1.0	0	1.0	2.5	0.34	30.85

TABLE 4
MONTE CARLO SIMULATION ESTIMATES FOR THE NON-DIMENSIONAL RADIATIVE HEAT FLUX q^*

Physical	K_a, K_s	$N_{w,1}$	q^*	
L,W,Z (m)	cm^{-1}		MC (MCTR.m)*	Reference Case (no scattering)
1,1,0.25	0.06,0.04	10^5	0.3404	0.3401
1,1,0.25	0.03,0.02	10^5	0.5002	0.5000
1,1,0.25	0.015,0.010	10^5	0.6587	0.6800
1,1,0.25	0,0	10^5	0.9997	1.0000

*MATLAB® program written

In the first case, the two black surfaces are at 2000 K and 0 K respectively. They have a surface area each of 1 m^2 and are separated by a distance 0.25 m. In the absence of a participating medium, the net heat flow is $F_{12}\sigma AT^4$ = 57.335 W/cm^2. With a participating medium $K_a = 0.06cm^{-1}$ $K_s = 0.04cm^{-1}$, and $t_L = 2.5$, q^*=0.34 [2] and $Q = q^* e_{b,1} = q^* \sigma AT^4 = 30.85$ W/cm^2.

Notice that the view factor (0.6320 in this case) does not enter the calculation. The MC estimate with the isotropic scattering and isotropic re-emission simulation, in Table 4, gives q^*=0.3404 and hence the same heat load of 30.85 W/cm^2. The accuracy of the estimates as a function of the number of batches N_B and the number of photon bundles simulated per batch N_P is listed in Table 5.

TABLE 5
ACCURACY OF MONTE CARLO SIMULATION ESTIMATES FOR THE NON-DIMENSIONAL RADIATIVE HEAT FLUX WITH THE NUMBER OF INDEPENDENT BATCHES AND PHOTON BUNDLES SIMULATED
$K_a = 0.06, K_s = 0.04$ CM^{-1}

S.No	N_B	N_P	$< q^* >$	σ_{q^*}
1	10	10	4.5000e-001	1.5652e-001
2	10	100	3.3300e-001	4.1243e-002
3	10	1000	3.3710e-001	1.5764e-002
4	10	10000	3.4084e-001	4.3502e-003
5	10	100000	3.4098e-001	1.4154e-003
6	20	100000	3.4040e-001	1.4415e-003

The present analysis can be applied for such situations to determine the effectiveness of candidate TBCs. including metals, semiconductors and dielectrics which can be used.

V. MC SENSITIVITY

A. Material Perturbations

To study the effect of material perturbation, we consider cases in which the independent parameters K_a, K_s are varied. Such work has been included in MC simulation for neutrons and photons, for example, in production codes such as MORSE [6] and MCNP [7]. The theory was demonstrated by Rief [9] and extended and applied in nuclear fusion reactor design sensitivity studies (see e.g. [10],[11.

In order to get some idea of the magnitude of change in the net heat flux due to a material perturbation, we carry out full re-runs when K_a alone is varied. The MC tallies are shown in Tables 6a and 6b.

TABLE 6A
MONTE CARLO SIMULATION ESTIMATES (RE-RUNS) FOR THE CHANGE IN RADIATIVE HEAT FLUX DUE TO A PERTURBATION IN THE MATERIAL ABSORPTION; BASE CASE $K_a = 0.06, K_s = 0.04$ CM^{-1}, *(1000X10)*

δK_a (%)	No. of Absorptions in Medium	No. of scatterings in Medium	$\delta t / t$ (%)	$\delta < q^* > / q_o^*$ (%)
-20	23815	19910	-12.0 (2.2)	+8.5
-10	26764	19692	-6.0	+3.7
0	29935	19857	0	0
10	33320	20232	+6.0	-4.0
20	35866	20051	+12.0 (2.8)	-7.0

TABLE 6B
MONTE CARLO SIMULATION ESTIMATES (RE-RUNS) FOR THE CHANGE IN RADIATIVE HEAT FLUX DUE TO A PERTURBATION IN THE MATERIAL SCATTERING; BASE CASE $K_a = 0.06, K_s = 0.04$ CM^{-1}, *(1000X10)*

δK_s (%)	No. of Absorptions in Medium	No. of scatterings in Medium	$\delta t / t$ (%)	$\delta < q^* >$ (%)
-20	30551	16397	-8 (2.30)	+6.4
-10	29759	17979	-4 (2.40)	+2.9
0	29935	19857	0 (2.50)	0
10	29526	21661	4 (2.60)	-2.8
20	29138	23333	8 (2.70)	-4.7

The thermal radiative transfer formulation is very similar to the neutron and photon transport as it based on the integral form of the Boltzmann equation. Traditionally, MC simulation is seen to be analogous to the Neumann series solution of the governing integral equation. Thus, we consider an idealized, extensively studied, 1-D slab transmission problem for which the exact solution is readily available (see e.g. [8]).

A simple demonstration of the perturbation method will be made by way of the slab transmission probability problem. A mono-energetic beam of photons is incident on the left side of the slab for which $K_a = 0.06, K_s = 0.04$ cm^{-1}, and the optical thickness is $t = K_t z$. For infinite parallel plates, the governing integral equation (Volterra equation of the second type) given above

$$I(t,\mu) = I(0,\mu)\exp(-t/\mu) + \int_0^t I_b(t')\exp(\frac{t'-t}{\mu})\frac{dt'}{\mu}$$

is considered, for the case of forward scattering i.e. $\delta(\mu - 1)$ and, initially, for a simpler model described by

$$I(t) = I(0)\exp(-t) + \int_0^t I_b(t')\exp(t'-t)dt' \equiv$$

$$S(t) + \int_0^t I(t')p_s \exp(t'-t)dt'$$

Mathematically, the integral equation can be solved by the Neumann series method as follows: assume initially that

$I(t) \equiv I_0(t) \cong S(t) = e^{-t}$, use this in the integral equation to get

$$I_1(t) = S(t) + e^{-t}\int_0^t dt_1 \equiv e^{-t} + \int_0^t S(t_1)K(t_1 \to t)dt_1$$ and use $I_1(t)$ to get a 'better' solution

$$I_2(t) = S(t) + e^{-t}\int_0^t dt_1\int_0^{t_1} dt_2 \equiv e^{-t} + \int_0^t\int_0^{t_1} dt_1 dt_2 S(t_1)K(t_1 \to t_2)K(t_2 \to t)$$

and so on.

The Neumann series analytical solution to the above can then be written as

$$I(t) = I(0)e^{-t} + \sum_{n=1}^{\infty} I_n(t)$$

where

$$I_n(t) = \int_0^t\int_0^{t_1}\Lambda \int_0^{t_{n-1}} dt_1 dt_2 \Lambda\ dt_n K(t_n \to t)\prod_{i=1}^{n-1} K(t_i \to t_{i+1})$$

In the above, the transition kernel $K(t_i \to t_{i+1})$ can be written as a 'collision' term $C_i = p_{s,i}$, the scattering probability at the i^{th} collision, and a 'transport' term $T(t_i \to t_{i+1}) = e^{-(t_{i+1}-t_i)}$ which transports the particle to the $(i+1)^{th}$ collision site. Thus the transition kernel is $K(t_i \to t_{i+1}) = C_i \cdot T_i$ where it is understood that C_i carries the pre-collision statistical 'weight' and properties of the particle, and T_i carries the post-collision information. This formulation, as will be shown in subsequent work, makes a perturbation analysis straight-forward. We can also attempt to write down a formulation for the stochastic process in which the random walk is treated in an analog manner with the only exception of allowing a particle to continue its 'history', or life, with a reduced 'weight' (equal to the pre-collision survival probability) even though it may actually have been absorbed. The complete set of events for a collision density or a transmission problem, whose probabilities must add up to unity, is then the contribution from events with zero collisions, with one collision, with two collisions and so on. When these are written, we will at once see the significance of the Neumann series solution which proceeded on purely mathematical grounds. The probabilities can be written as:

$$P_T(0 \mid T) = e^{-T}$$

$$P_T(1 \mid T) = \int_0^t dy_1 e^{-y_1}\cdot e^{-(T-y_1)} = e^{-T}\int_0^T dy_1 = e^{-T}T$$

$$P_T(2 \mid T) = \int_0^T dy_1 e^{-y_1}\cdot\int_{y_1}^T dy_2 \cdot e^{-(T-y_2)} = e^{-T}\frac{T^2}{2!}$$

$$P_T(3 \mid T) = \int_0^T dy_1 e^{-y_1}\cdot\int_{y_1}^T dy_2 \cdot e^{-(y_2-y_2)}\int_{y_2}^T dy_3 \cdot e^{-(T-y_3)} = e^{-T}\frac{T^3}{3!}$$

$$\Lambda$$

$$P_T(n \mid T) = e^{-T}\int_0^T dy_1\int_{y_1}^T dy_2 \Lambda \int_{y_n}^T dy_n = e^{-T}\frac{T^n}{n!}$$

The exact solution for the collision density and the transmission probability can then be found as $\psi(t) = \sum_{n=0}^{\infty} p^n e^{-t}\frac{t^n}{n!} = e^{-(K_a/K_t)t}$ and $J((T) = e^{-(K_a/K_t)T}$ respectively. Since $t \equiv K_t z$ and $T \equiv K_t Z_o$, $\psi(t) = \exp(-K_a z)$, and $J(T) = \exp(-K_a Z_o)$, and the change in each quantity due a material change δK_t has an exact solution $\delta\psi/\psi = -z\delta K_t$ and $\delta J/J = -Z_o\delta K_t$ respectively. Following a simulation, the estimator for a first derivative for ψ is then obtained as $<\delta\psi> \cong < p^n\left\{(\frac{n}{t}-1)\delta t + \frac{n}{p}\delta p\right\} >$ where the estimate is obtained in a single 'run'. To test the accuracy of this estimate, we carry out simulations in the following stages:

i- carry out a simulation to estimate $<\psi>, \sigma_{<\psi>}$ and $<J(T)>, \sigma_{<J>}$

ii- compare above with exact results

iii- construct a PDF, $<P(n \mid Z_o)>$ and compare with a Poisson PDF

iv- carry out full re-runs for a specified $\delta K_t / K_t$ (±5%,±10%)

v- show changes in Poisson PDFs for the material perturbation

vi- use the estimator in a single run to 'predict' changes in $<\delta\psi>$

The MATLAB® program MCslab.m was used for simulation, construction of a PDF from the simulation for the transmission through the last surface, and for comparison with the exact analytical solution for the collision density obtained from the integral equation.

The figure below shows a simulation for a slab of $t = 10$ (optical thickness) with 20 regions, *i.e.* 0.5 optical thickness each. Since $< t >= 1$, the probability of having a collision in a region is small and the CE is bound to give an inaccurate result. This is illustrated in the figures below for a sample size of 1000X5. The discrepancy remains even as the sample size is increased to 100000X5. However, the results improve as the size of the regions is increase from 0.5 to 1.0 optical units. For the CE to provide reliable results in an MC simulation, the size of the region, or mesh in a deterministic analogy, must be larger than an optical unit. In case the mesh size can not be increased, the track-length estimator (TLE) should be used instead of the CE.

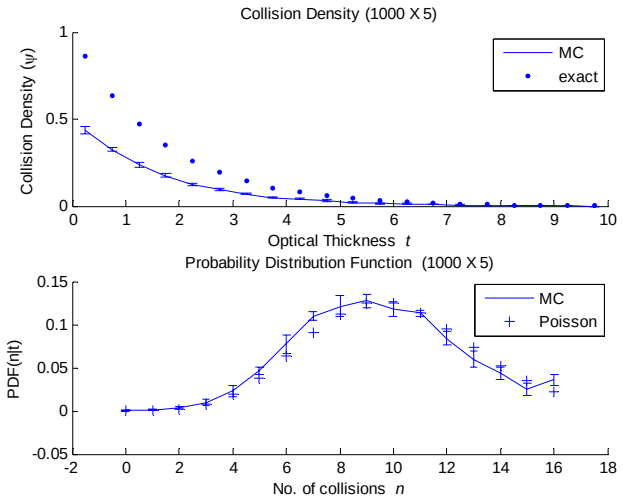

Fig. 1. Monte Carlo simulation, 1000 particles and 5 batches, for a 1-D slab of thickness 10 optical units, with forward scattering and 20 regions.

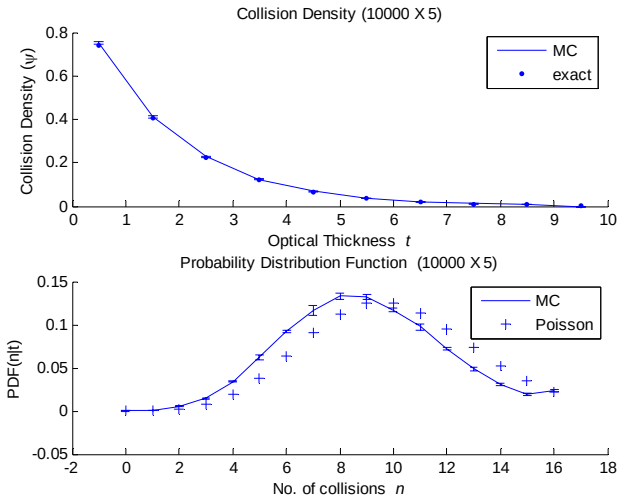

Fig. 2. Monte Carlo simulation, 10000 particles and 5 batches, for a 1-D slab of thickness 10 optical units, with forward scattering and 10 regions.

As discussed above, the estimator for a first derivative for ψ is obtained as

$$< \delta\psi > \cong < p^n \left\{ (\frac{n}{t} - 1)\delta(t) + \frac{n}{p}\delta(p) \right\} >$$

where the estimate is obtained in a single 'run'.

VI. Conclusion

We have carried out a comparison of two deterministic methods with Monte Carlo analog simulation for computing the radiative flux for flat isothermal plates and have shown the effort required in each method. While MC is computation-intensive, it has the advantage of being applied to complex geometrical configurations and is capable of handling realistic scattering laws for thermal radiation. This is a great advantage over deterministic methods. We have also considered the MC random-walk in some detail to show the approach by which derivative quantities can be sampled during a full simulation. This work is useful as a didactic exercise to extend MC to complex problems for engineering design sensitivity.

References

[1] J. P. Holman, *Heat Transfer*, Seventh Edition, McGraw-Hill Inc., 1992.
[2] M. Quinn Brewster, *Thermal Radiative Transfer and Properties*, John Wiley & Sons, Inc., 1992.
[3] Michael F. Modest, *Radiative Heat Transfer*, Second Edition, Academic Press, 2003.
[4] Gökmen Demirkaya, Monte Carlo Solution of a Radiative Heat Transfer Problem in a 3-D Rectangular Enclosure Containing Absorbing, Emitting, and Anisotropically scattering medium, M.S. Thesis, Department of Mechanical Engineering, Middle East Technical University, December 2003.
[5] J. Spanier and E. M. Gelbard, *Monte Carlo Principles and Neutron Transport Problems*, Addison-Wesley Publishing Company, 1969.
[6] E. A. Straker, P. N. Stevens, D. C. Irving and V. R. Cain, The MORSE Code – A Multigroup Neutron and Gamma-ray Monte Carlo Transport Code, Oak Ridge National Laboratory, ORNL-4585 (1970)
[7] J. F. Briesmeister, Ed., "MCNP—A General Monte Carlo Code for Neutron and Photon Transport", LA-7396-M, Los Alamos National Laboratory (1986).
[8] M. Ragheb, Slowing Down in Hydrogen or Particle Transmission through a Slab Shield, University of Illinois, Urbana-Champaign, 2003.
[9] H. Rief, "Generalized Monte Carlo Perturbation Algorithms for Correlated Sampling and a Second-Order Taylor Series Approach", Annals of Nuclear Energy, vol. 11, 9, 455 (1984).
[10] Z. U. Koreshi and J. D. Lewins, "Two-group Monte Carlo Perturbation Theory and Applications in Fixed-Source Problems", *Progress in Nuclear Energy*, vol. 24, pp.27-38 1990.
[11] Z. U. Koreshi, A. Kinrot and J. D. Lewins, "Neutronic Sensitivity Analysis of the Experimental Test Reactor TIBER-II Blanket Design", *Fusion Technology*, vol. 22, No.3, pp.371-387, Nov.1992.